CGU HS Committee on River Ice Processes and the Environment
17th Workshop on River Ice
Edmonton, Alberta, July 21 - 24, 2013

Measuring supercooling prevalence on small regulated and unregulated streams in New Brunswick and Newfoundland, Canada

Jennifer Nafziger[1*], Faye Hicks[1], Paula Thoms[2], Vincent McFarlane[1], Janelle Banack[1], and Richard A. Cunjak[2]

[1]*University of Alberta, Department of Civil Engineering, Edmonton, AB T6G 2W2*
**jnafzige@ualberta.ca*

[2]*Canadian Rivers Institute, Department of Biology, University of New Brunswick, Fredericton, NB E3B 5A3*

Supercooling is difficult to measure in the field as the degree of supercooling that occurs in natural waters is in the order of a few hundredths of a degree Celsius. Given the high cost of the most accurate water temperature sensors, four types of sensors were compared to an accurate reference sensor to determine if they could detect supercooling events at small temperature scales. All tested sensors were able to do so, but with varying degrees of error from the reference sensor. The use of a residual temperature measured in the field as a threshold temperature is proposed as a method to gain supercooling information from less accurate sensors. Supercooling data were thus derived from a data set collected on small regulated and unregulated streams in Newfoundland and New Brunswick. Supercooling was observed in the six study sites, occurring 11 to 52 times per season, with a maximum degree of supercooling of 0.07°C below the assumed reference temperature datum. Measured supercooling events lasted for up to 42.7 hours.

1. Introduction

Supercooling is necessary to form frazil ice, and is therefore fundamental to understanding river ice processes. Supercooling events are important to detect and predict because the resulting frazil production can lead to blockages at municipal and industrial facilities (e.g. Richard and Morse, 2008; Ettema et al., 2009). Supercooling and frazil ice may also affect winter fish survival (Brown, et al., 2011, Brown, et al., 1999) and cold temperatures may significantly reduce salmonid embryo survival (e.g. Tang, et al., 1987). Supercooling is difficult to measure in the field as the degree of supercooling that occurs in natural streams is typically in the order of a few hundredths of a degree Celsius. The presence and the amount of supercooling have been measured in the laboratory (e.g. Clark and Doering, 2006); however, few continuous field-based measurements exist in the literature (e.g. Richard and Morse, 2008; Morse and Richard, 2009) and no such data sets exist for an entire season or on small, steep streams where salmonid spawning is likely.

This paper presents an analysis of supercooling events measured over an entire season on small streams in Newfoundland and New Brunswick. These data were collected using Vemco Minilog-II-T water temperature sensors, which have an accuracy error cited by the manufacturer of 0.1°C. Generally, an accuracy error of 0.01°C or better is required to measure supercooling. In order to analyze the field data for supercooling events, a series of laboratory calibration experiments were performed to compare the Vemco Minilog-II-T sensors to a more accurate sensor. Given the high cost of accurate sensors and the high risk of loss or damage under ice-affected conditions, the ability of three other common water temperature sensors to resolve supercooling events was also investigated.

2. Background

Supercooling during frazil formation was described by Osterkamp (1978) and Michel (1978). Figure 1 is a schematic showing a supercooling event resulting from a constant rate of heat loss, and illustrates the variables used in this paper. Supercooling occurs when the water temperature drops below the phase equilibrium temperature (T_e). In natural streams this temperature is close to zero degrees Celsius, but depends on pressure and solute concentration according to the following equation (Osterkamp, 1978):

$$T_e = 0.0100°\text{C} + T_P - 1.86m \qquad [1]$$

where:

T_e = phase equilibrium temperature of water, °C;
0.0100 = the triple point of water, °C;
T_p = pressure correction; and
m = solute concentration, molaity.

The phase equilibrium temperature also depends on the curvature of the surface between the phases, but this can be ignored for water-to-ice phase changes (Osterkamp, 1978).

As water cools due to a constant rate of heat loss, the temperature change is governed by Equation 2:

$$\frac{dT}{dt} = \frac{\phi}{cM_w} + \frac{L}{cM_w}\frac{dM_i}{dt} \qquad [2]$$

where:

T	=	temperature;
t	=	time, referenced to any origin;
ϕ	=	net heat transfer from water, losses are negative;
c	=	specific heat of water at a constant pressure;
M_w	=	mass of water;
L	=	latent heat of fusion; and
M_i	=	mass of ice.

At temperatures above T_e, only liquid water is present, and M_i is therefore zero. As the water cools below T_e, the water is considered supercooled. At some point in time (termed t_n, the time of nucleation), frazil ice will start to form and dT/dt decreases as heat is gained by the water from the latent heat of fusion. As nucleation continues, the terms on the right hand side of Equation 2 will eventually become equal, as heat loss is balanced by heat gained from ice formation. After this point the water temperature is called the residual supercooling temperature (T_r).

3. Laboratory Calibration

3.1 Methodology

Five water temperature sensor types were compared in the laboratory. The accuracy error, precision error, response time, and drift of each type of sensor, as cited by the manufacturers, are presented in Table 1. The SeaBird SBE39 was chosen as the reference sensor. It is highly accurate (± 0.002ºC) and was available for each calibration. Several sensors of each type were compared to the single reference sensor: two Vemco Minilog-II-T, 12 Onset HOBO TidbiTv2, 8 RBR RBRSoloT, and 26 Schlumberger Diver sensors – a combination of MiniDivers (model DI501) and MicroDivers (model DI601). The two Schulmberger models are treated as a single sensor type in this analysis.

Rather than simply testing the instruments in a thermal bath to generate a calibration curve, the approach used in this study was to determine if the instruments could resolve the features of the typical supercooling curve shown in Figure 1. This was achieved during actual supercooling and

frazil generation experiments conducted in the 0.8 m x 1.2 m x 1.5 m (width x length x depth) frazil tank at the University of Alberta Cold Room Facility (Ghobrial et al., 2009). Each type of sensor was tested in a separate experiment. Figure 2 illustrates how the sensors were fixed in the tank; the SeaBird SBE39 and the Schlumberger Divers were fixed to a custom-designed frame, whereas the other sensors were simply tied to the frame. The sensors' internal clocks were synchronized to Microsoft Windows internet clock time. They were then set to record water temperatures at different time intervals depending on their programming capabilities and memory capacity: the SeaBird SBE39 sensor was set to record at one or two second intervals; the Vemco Minilog-II-T sensors recorded data at five second intervals; the RBRSoloT sensors recorded every second; and the Schlumberger Diver and HOBO TidbiT sensors recorded data every minute. For each experiment, the cold room air temperature was set at approximately -10°C and the propellers in the tank were turned on to generate a turbulent environment. The temperature sensors recorded the water temperature while (1) the water cooled, (2) the water supercooled, (3) frazil ice was generated, and (4) the temperature stabilized. After the water temperature was stable for at least an hour, the experiment was ended, the sensors removed from the tank, and the data were downloaded.

3.2 Results and Analysis

Figure 3 illustrates the two parameters used to determine the effectiveness of each sensor in characterizing a supercooling event: (1) the maximum supercooling below the residual supercooling temperature ($\Delta T_{r\text{-}max}$), and (2) the duration of temperature below the residual supercooling temperature (Δt_{rs}). These parameters were chosen because they are of interest when characterizing supercooling and frazil ice formation events in the field. Both parameters are referenced to the residual supercooling temperature (T_r) and not to the phase equilibrium temperature (T_e), as the phase equilibrium temperature is difficult to quantify accurately. In particular, Osterkamp (1978) cautioned against calculating T_e from Equation 1 using measured solute concentrations because incomplete dissociation of salts and neutral molecules of sulfates and carbonates in natural waters may cause errors. In contrast, the residual supercooling temperature, T_r, is easily quantified from experimental temperature data. Having a relative value against which to reference parameters also allows for the use and comparison of sensors whose offset from zero has drifted or is inaccurate.

Data from each individual sensor were compared to the reference sensor. For simplicity, the differences between the reference sensor and the test sensors are referred to as "error." However, data from the reference sensor itself may contain inaccuracies, and do not necessarily represent the true water temperature. The curve for each sensor was analyzed, the residual supercooling temperature (T_r) was determined and $\Delta T_{r\text{-}max}$ and Δt_{rs} were calculated. The percent error in $\Delta T_{r\text{-}max}$ and Δt_{rs} were then calculated for each sensor. The temperature offset error, ΔT_e, was estimated for each sensor, based on the average difference in T_r measured by that sensor and the reference sensor; it was then used as the temperature offset correction for that sensor.

Figure 4 shows representative results for each type of sensor tested. In this figure, the data from the test sensors have been corrected for ΔT_e. In addition, for ease of visual comparison, errors in syncing the individual sensor clocks were neglected by aligning the measured minimum water temperatures for each with the minimum temperature recorded by the reference sensor. Once corrected for ΔT_e, even those sensors with relatively large accuracy errors of 0.1°C and 0.2°C (Table 1) were able to resolve a supercooling dip in temperature of less than 0.1°C. However, other sensor attributes (i.e. precision, response time) may have affected the ability of the sensors to usefully resolve the feature of the supercooling curve. For example, because of their large precision error (0.02°C) and long response time (5 minutes) the HOBO TidbiT sensors frequently underestimated $\Delta T_{r\text{-}max}$. Most sensors more accurately captured the cooling section of the supercooling curve, where *dT/dt* is fairly constant, than the later (warming) section. The HOBO TidbiTs and Schlumberger Divers tended to show a slower warming than did the reference sensor, and therefore overestimated Δt_{rs}. The longer response times of these sensors may account for this. For example, the RBRSoloT with its low precision error (0.0001°C) and short response time (1 second) performed best in detecting the duration of supercooling (t_{rs}).

Table 2 provides the average, maximum, and minimum errors in $\Delta T_{r\text{-}max}$, Δt_{rs}, and ΔT_e for each type; Figures 5 and 6 summarize these results graphically. As Figure 5 illustrates, the RBRSoloT and the Vemco Minilog-II-T sensors performed best, having the lowest average percent error in both parameters (4.4% to 11.3%). The Schlumberger Divers performed worst, with the highest average percent error in Δt_{rs} of 20.9%. As seen in Figure 6, the RBRSoloT and the Vemco Minilog-II-T also had the lowest offset errors (ΔT_e of 0.005°C and 0.030°C, respectively). The Schlumberger Divers had the highest average ΔT_e (0.094°C); however, this high average was primarily due to 3 individual sensors with particularly large values of ΔT_e (0.730°C maximum). If these three sensors are neglected in calculating the average ΔT_e for the Schlumberger Divers, the value for the remaining instruments is only 0.050°C. Based on the results presented in this section, data from Vemco Minilog-II-T were considered accurate enough to detect supercooling. Field data using Vemco Minilog-II-T sensors are analyzed in the following sections.

4. Field Deployment

4.1 Methodology

Vemco Minilog-II-T sensors were installed in five study streams to collect water temperature data over the winters of 2010-2011 (Newfoundland) and 2011-2012 (New Brunswick). These data were collected as part of a larger Natural Sciences and Engineering Research Council (NSERC) HydroNet research project investigating the combined effects of winter stressors (e.g. water temperature, ice processes, water chemistry) on the winter survival of Atlantic salmon (*Salmo salar*) embryos and how those stressors may differ between regulated and unregulated

streams. Figures 7 and 8 show the location of the study sites in Newfoundland and New Brunswick, respectively. These included sites in two streams in Newfoundland (West Salmon River and Twillick Brook) and in three streams in New Brunswick (River Dee, Serpentine River, and Gulquac River). Twillick Brook and Gulquac River are natural flow (unregulated) streams, while the other three streams (West Salmon River, River Dee and Serpentine River) are regulated and located downstream of headpond storage dams. Sensors were installed at two sites on the Gulqac River, and at one site in each other stream. Each sensor was attached by a plastic-coated cable to a cinder block, which was, in turn, tethered to the stream bank. The sensors were installed in October, before the ice-affected season, and retrieved the following May or June; each was programmed to record water temperatures at one or two minute intervals throughout that time period.

4.2 Results and Analysis

In natural rivers, the rate of heat loss cannot be considered constant over a long period of time, as meteorological, ice cover, stream flow, and groundwater conditions all change with time. Figure 9 is a schematic showing a representative supercooling event in a natural river. Here, a consistent T_r may not be reached after each supercooling event, and the value of T_r may change with each event, or during an event. Therefore, a different threshold parameter must be used to separate supercooled temperatures from non-supercooled temperatures. The threshold parameter used in the following analysis is termed the "field residual temperature" (T_r'), defined as the minimum consistent temperature measured over the season. It is expected that T_r' (if corrected for instrument error) has a value between T_e and T_r, and therefore can be used as the threshold temperature that defines supercooling. This analysis assumes consistent water chemistry over the winter season at a site. Field supercooling events were characterized by their maximum supercooling below the field residual temperature ($\Delta T_{r\text{-}max}$') and the duration of the event below the field residual temperature (Δt_{rs}'). Each sensor at a site has a unique T_r'; since $\Delta T_{r\text{-}max}$' and Δt_{rs}' are measured relative to this value, the need to correct for instrument offset error (ΔT_e) is eliminated.

Supercooling events were detected in the continuous winter water temperature data collected at the six study sites. Figure 10 shows the water temperature data for site G1 on the Gulquac River in New Brunswick and is representative of the type of data collected. Typically, water temperatures fluctuated widely in the autumn, then decreased to a relatively consistent T_r' during the main ice-covered season, and then fluctuated widely again in the spring. Supercooling events occurred throughout the autumn, winter, and spring, but were most common just before and after the main ice-affected season. A supercooling event was defined as a water temperature below T_r' for more than five minutes. If events were less than 60 minutes apart, they were counted as a single event. In this case, only the time the water temperature was below T_r' was counted towards the duration of the event. For each supercooling event T_r', $\Delta T_{r\text{-}max}$', and Δt_{rs}' were determined. Figures 12 and 13 illustrate these parameters at site D3 on the River Dee. Figure 11

shows an entire season of low temperatures. Here, T_r' was determined to be -0.02°C, the minimum consistent temperature during the ice-affected season. In Figure 11, supercooling events appear as downward spikes. Figure 12 shows a detailed view of a single supercooling event at site D3, showing a T_r' of -0.02°C, a $\Delta T_{r\text{-}max}$' of 0.06°C, and a Δt_{rs}' of 1.8 hours.

Table 3 and Figures 13, 14, and 15 summarize the supercooling events for each site. On the Newfoundland sites, supercooling was significantly more pronounced at the Twillick Brook site than at the West Salmon River site. Twillick Brook had more frequent (Figure 13), colder (Figure 14), and longer duration (Figure 15) supercooling events. This is likely because the West Salmon River site (Site WS1) is located close (~500 m) to the outfall of the West Salmon Dam, and the site is influenced by warm hypolimnion water being released from the reservoir. The patterns are less clear for the New Brunswick sites. Site D3 on the regulated River Dee had the smallest number of supercooling events (26), had the second largest maximum degree of supercooling ($\Delta T_{r\text{-}max}$') of 0.06°C, and had intermediate duration of events (Δt_{rs}') (maximum 14.9 hours). Site S3 on the regulated Serpentine River had the second largest number of supercooling events (43), was tied for the smallest $\Delta T_{r\text{-}max}$' with Site G3 of 0.04°C, and had the shortest Δt_{rs}' (maximum 7.3 hours). Site G1 on the unregulated Gulquac River had the smallest number of supercooling events (22), had the largest $\Delta T_{r\text{-}max}$' of 0.07°C, and had an intermediate Δt_{rs}' (maximum 14.2 hours). Site G3 on the unregulated Gulquac River had the largest number of supercooling events (52), and had the longest Δt_{rs}' (maximum 42.7 hours).

In the spring, the daytime warming of the water temperature did not allow the water to stabilize at a T_r'. For example, Figure 16 shows supercooling events at Site G1 on the Gulquac River. From March 31 to April 3, 2012 supercooling occurred every morning with the water temperature rising each day. This prevented the water temperature from equilibrating at T_r'. If the data collected were only of a fluctuating regime like this (e.g. for a hydropeaking regime, tidal regime, or for a short spring data set) the value of T_r' could not be established, and sensors with an accuracy of better than 0.01°C would have to be used to characterize the supercooling regime.

These supercooling data should be further analyzed in conjunction with available camera-derived ice condition and meteorological data. This could answer some intriguing questions such as: Is supercooling possible under an ice cover? What are the causes of any midwinter supercooling events? Are snowfall-derived frazil events accompanied by supercooling?

5. Conclusion

The water temperature sensors tested here are capable of detecting and resolving supercooling events, despite the broad accuracies reported by their manufactures. Field and laboratory water temperature data can be analyzed using a relative datum, assuming the water temperature environment is relatively stable. Supercooling was observed in the six study sites, occurring 11

to 52 times per season, with a maximum degree of supercooling of 0.07°C below the assumed reference temperature datum. Measured supercooling events lasted for up to 42.7 hours.

6. Acknowledgements

The authors would like to thank the Natural Sciences and Engineering Research Council of Canada's (NSERC) for funding this research through the NSERC HydroNet network, research grants, and graduate scholarships.

7. References

Brown, R.S., Hubert, W.A., and Daly, S.F. 2011. A primer on winter, ice, and fish: What fisheries biologists should know about winter ice processes and stream-dwelling fish. *Fisheries*. 36:1. 8-36.

Brown, R.S., Brodeur, J.C., Power, G., Daly, S.F., White, K.D., and McKinley, R.S. 1999. Blood chemistry and swimming activity of rainbow trout exposed to supercooling and frazil ice. *10th Workshop on the Hydraulics of Ice Covered Rivers.* Winnipeg, MB. 97-110.

Clark, S., and Doering, J. 2006. Laboratory experiments on frazil-size characteristics in a counterrotating flume. *Journal of Hydraulic Engineering*. 132:1. 94-101.

Ettema, R., Kirkil, G., and Daly, S. 2009. Frazil ice concerns for channels, pump-lines, penstocks, siphons, and tunnels in mountainous regions. *Cold Regions Science and Technology*. 55:2. 202-211.

Ghobrial, T., Loewen, M., and Hicks, F. 2009. Frazil ice measurements using the shallow water ice profiling sonar. *15th Workshop on River Ice*. St. John's, Newfoundland.

Michel, B. 1978. *Ice Mechanics*. Les Presses De L'Université Laval.

Morse, B., and Richard, M. 2009. A field study of suspended frazil ice particles. *Cold Regions Science and Technology*. 55:1. 86-102.

Osterkamp, T.E. 1978. Frazil formation: A review. *ASCE Journal of the Hydraulics Division*. 104:9. 1239-1255.

Richard, M., and Morse, B. 2008. Multiple frazil ice blockages at a water intake in the St. Lawrence River. *Cold Regions Science and Technology*. 53:2 131-149.

Tang, J., Bryant, M.D., and Brannon, E.L. 1987. Effect of temperature extremes on the mortality and development rates of coho salmon embryos and alevins. *The Progressive Fish-Culturist*. 49:3. 167-174.

Tables

Table 1. Accuracy data for water temperature sensors tested in this study. (Source: documentation for each model, available from their manufacturers' respective website).

Manufacturer	Model	Accuracy Error (°C)	Data Precision (°C)	Response Time / Time Constant	Temperature Drift (°C)	Clock Drift
SeaBird Electronics, Inc.	SBE39	0.002	0.0001	25 seconds	~ 0.0002 per month	5 seconds per month
Vemco	Minilog-II-T	0.1	0.01	< 5 minutes to 90%	not specified	1 minute per month
RBR Ltd.	RBRSoloT	0.002	0.00005	1 second	~ 0.002 per year	1 minute per year
Schlumberger Ltd.	Mini- and Micro-Diver pressure transducers (DI 501/ DI 601)	0.1	0.01	not specified	not specified	1 to 5 minutes per year
Onset Computer Corporation	HOBO TidbiTv2	0.2	0.02	5 minutes	0.1 per year	1 minute per month

Table 2. Summary of experimental results comparing test sensors against a reference sensor (SeaBird SBE39) under supercooling conditions.

		Vemco MiniLog-II-T	RBR RBRSoloT	Schlumberger Diver DI501/DI601	Onset HOBO TidbiTv2
Number of sensors		2	8	26	12
Maximum supercooling below residual supercooling temperature ($\Delta T_{r\text{-}max}$) - percent error from reference sensor	Average	11.3	10.5	7.6	16.8
	Maximum	19.4	7.6	30.9	17.8
	Minimum	3.2	12.7	4.7	16.3
Duration of temperatures below residual supercooling temperature (Δt_{rs}) - percent error from reference sensor	Average	9.7	4.4	20.9	16.3
	Maximum	14.2	8.8	37.5	54.6
	Minimum	5.2	2.8	0.0	3.1
Absolute error from reference sensor (ΔT_e) (◦C)	Average	0.030	0.005	0.094	0.054
	Maximum	0.056	0.003	0.730	0.102
	Minimum	0.004	0.007	0.000	0.009

Table 3. Summary of supercooling events in the study streams in New Brunswick (2011-12) and Newfoundland (2010-2011).

Site	D3	S3	G1	G3	WS1	TB1
Province	New Brunswick				Newfoundland	
Stream	River Dee	Serpentine River	Gulquac River	Gulquac River	West Salmon River	Twillick Brook
Stream Type (regulated/ unregulated)	regulated	regulated	unregulated	unregulated	regulated	unregulated
Total # of Events	26	43	22	52	11	41
Average duration of supercooling, Δt_{rs}' (hours)	3.4	2.4	3.8	8.5	2.2	6.3
Minimum duration of supercooling Δt_{rs}' (minutes)	12	12	48	6	16	16
Maximum duration of supercooling, Δt_{rs}' (hours)	14.9	7.3	14.2	42.7	9.0	15.7
Maximum Supercooling ($\Delta T_{r\text{-}max}$', °C)	0.06	0.04	0.07	0.04	0.02	0.04

Figures

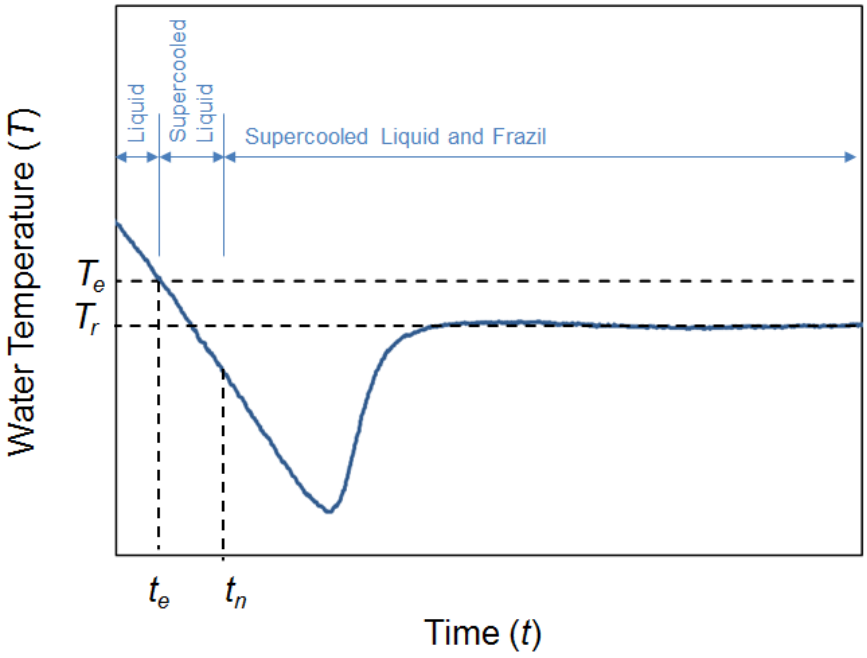

Figure 1. Schematic of a supercooling event for a constant rate of heat loss, T_e = phase equilibrium temperature, t_e = time of phase equilibrium temperature, t_n = time of nucleation, T_r = residual supercooling temperature.

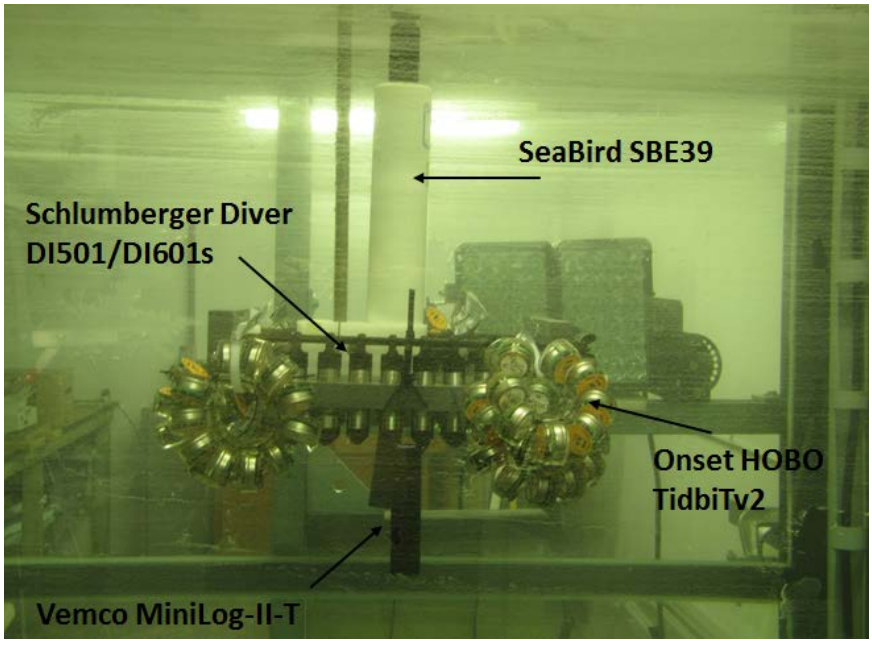

Figure 2. Example of how water temperature sensors were fixed in the frazil tank for the calibration experiments.

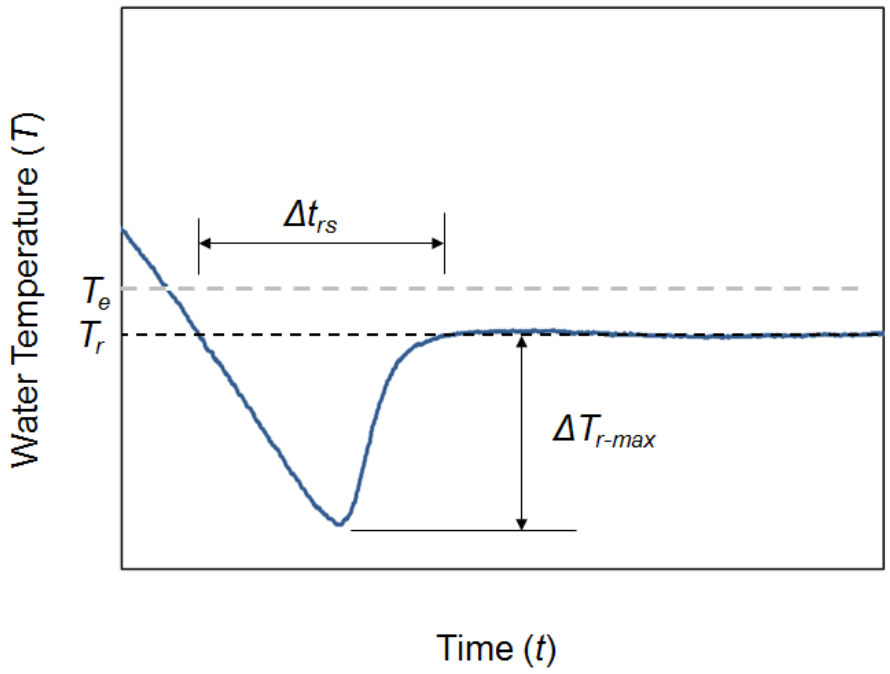

Figure 3. Schematic of a supercooling event for a constant rate of heat loss, showing variables used to evaluate the water temperature sensors tested in the laboratory: $\Delta T_{r\text{-}max}$ = maximum supercooling below residual supercooling temperature, Δt_{rs} = duration of temperatures below residual supercooling temperature.

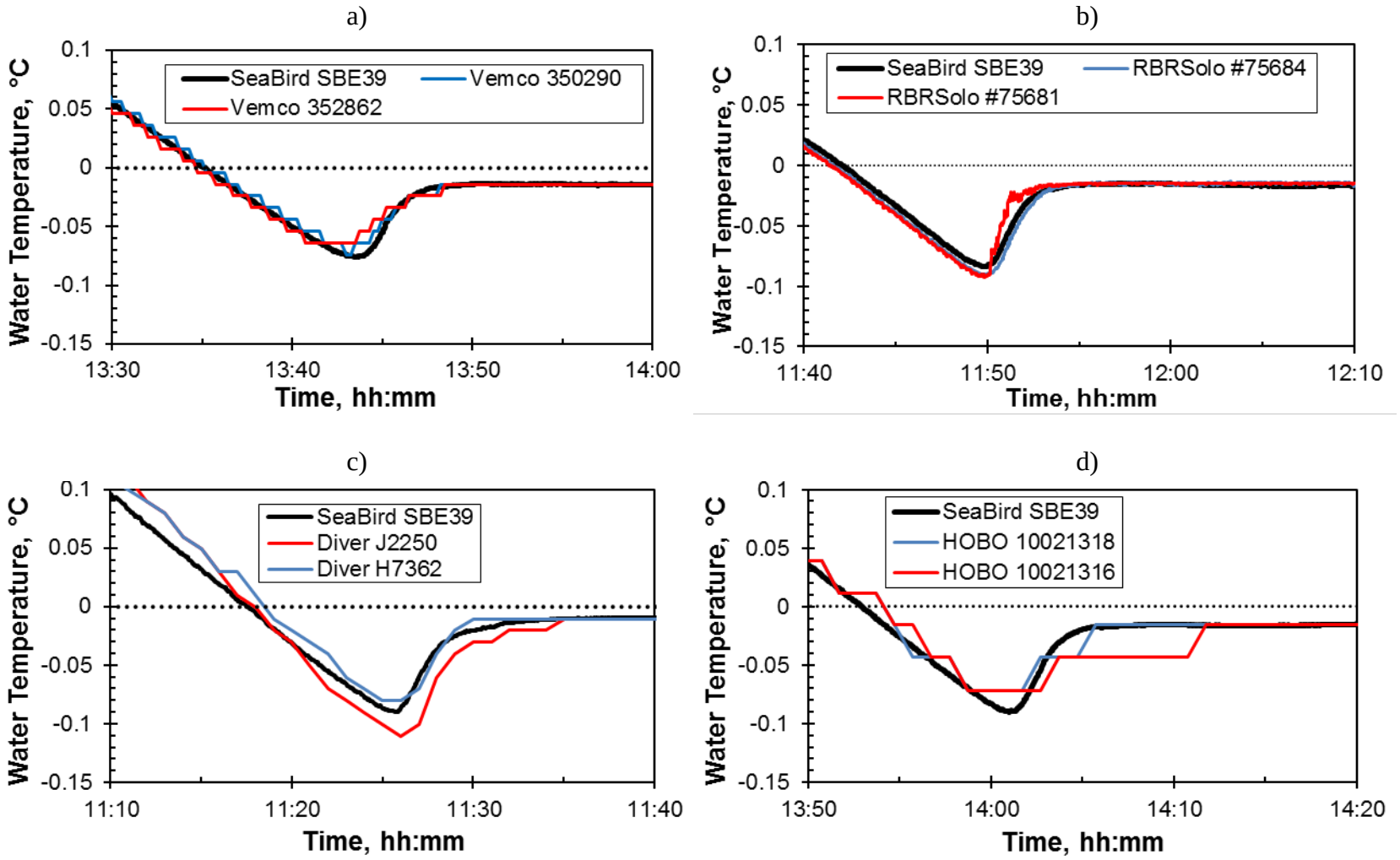

Figure 4: Summary of results of calibration experiments showing example data from each test type: a) Vemco Minilog-II-T b) RBRSoloT c) Schlumberger Diver DI501/DI601 d) HOBO TidbiTv2; test sensor data has been corrected for offset error (ΔT_e).

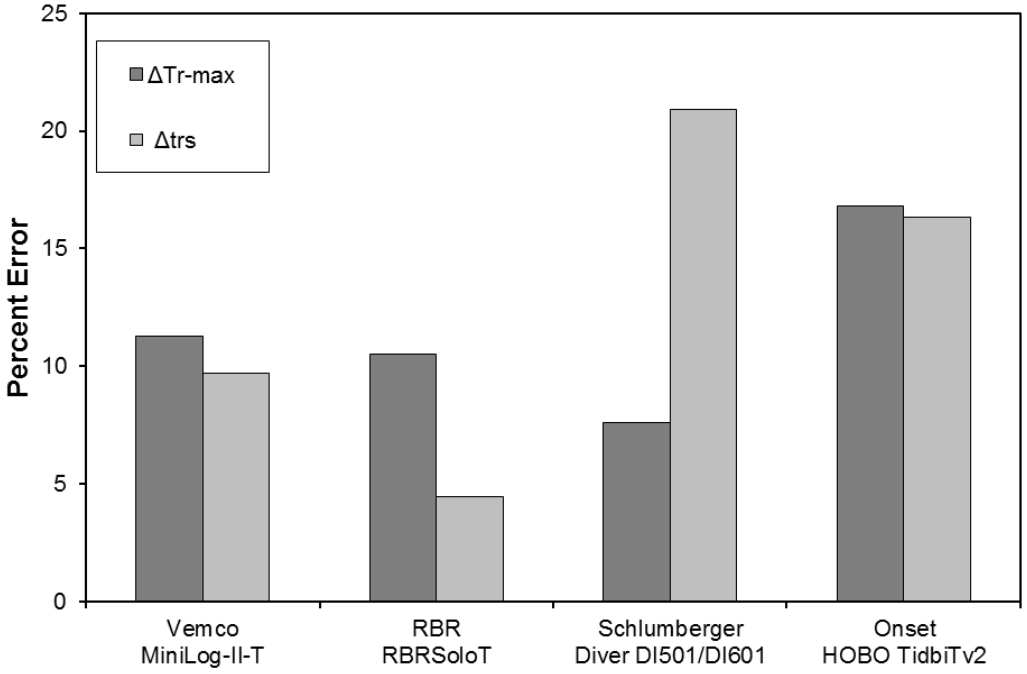

Figure 5. Summary of performance of test sensors in characterizing the maximum supercooling below residual supercooling temperature ($\Delta T_{r\text{-}max)}$ and duration of temperatures below residual supercooling temperature (Δt_{rs}); performance is expressed as average percent error compared to the reference sensor.

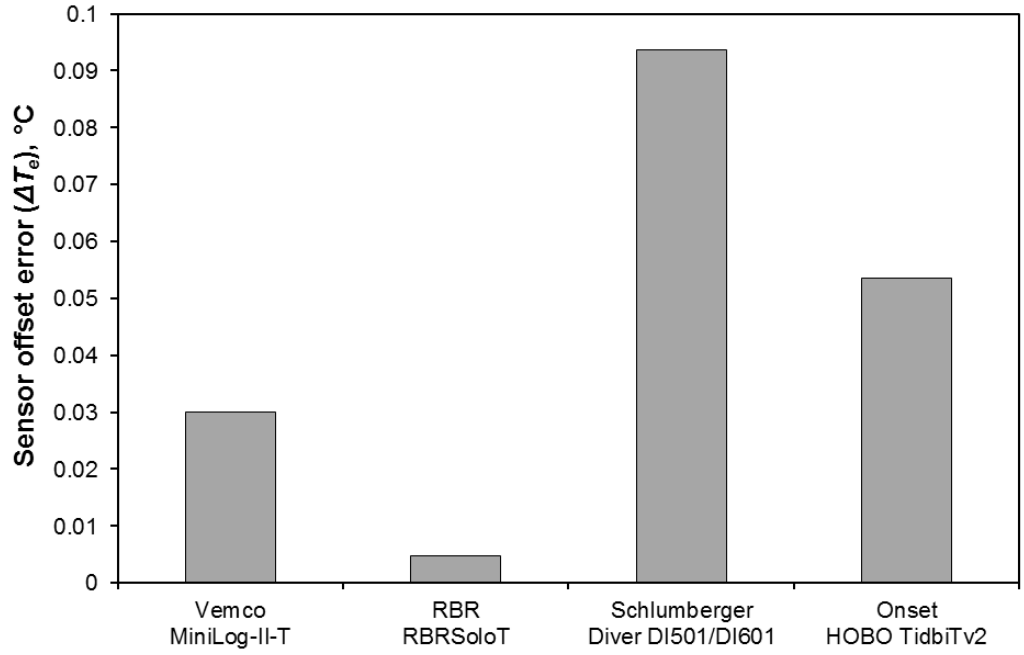

Figure 6. Summary of average temperature offset errors (ΔT_e) for each sensor type as compared to the reference sensor (SeaBird SBE39).

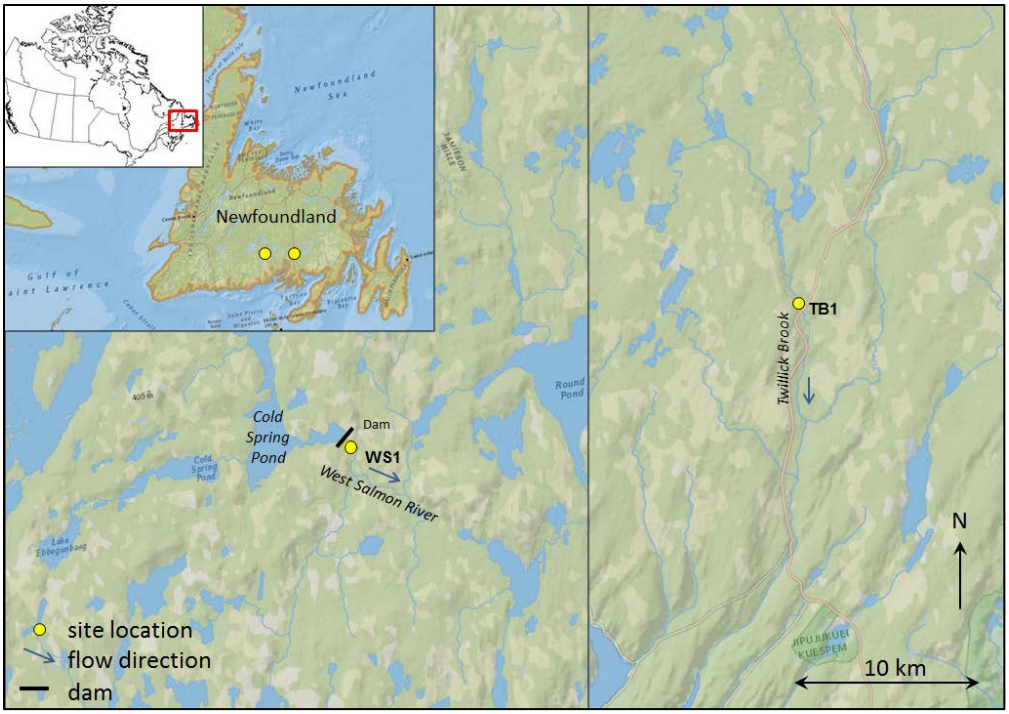

Figure 7. Site locations in Newfoundland, Canada (base image from ESRI ArcMap basemaps).

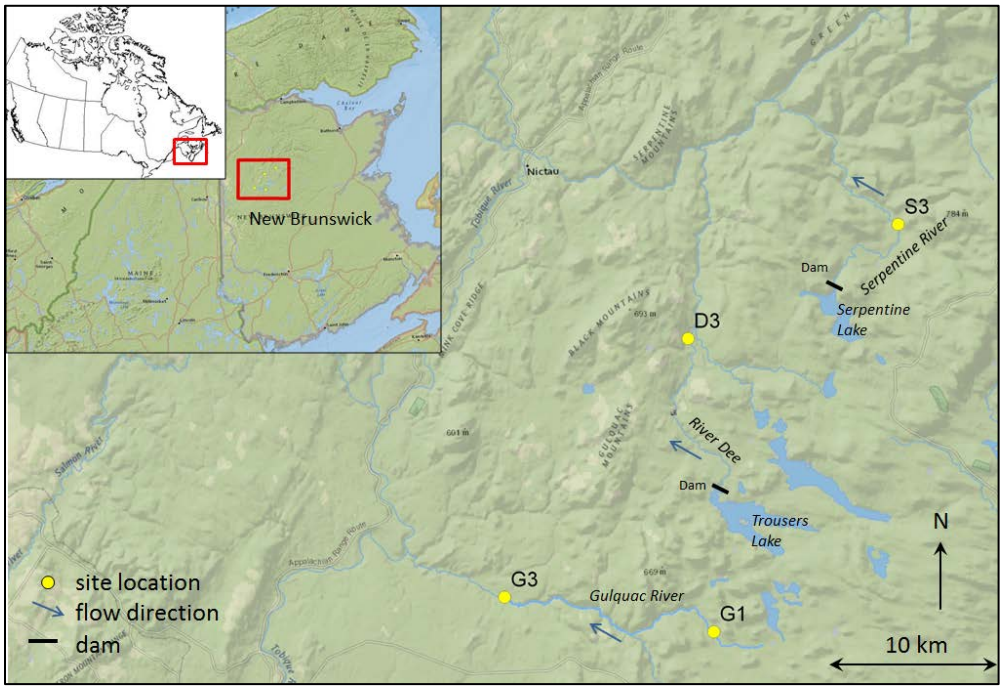

Figure 8. Site locations in New Brunswick, Canada (base image from ESRI ArcMap basemaps).

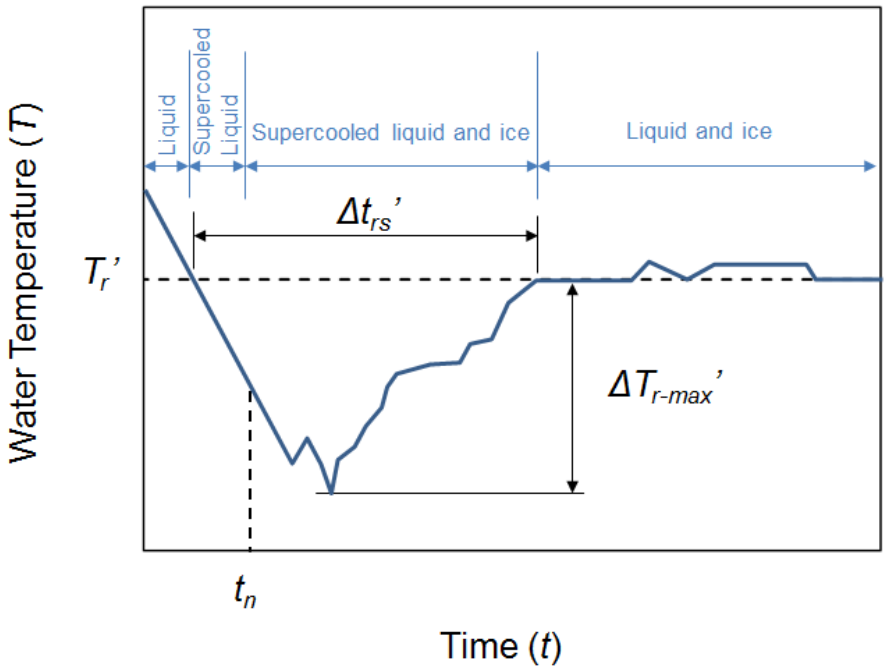

Figure 9. Schematic of a supercooling event under field conditions where heat loss is not constant: T_r' = field residual temperature, t_n = time of nucleation, $\Delta T_{r\text{-}max}$' = maximum supercooling below field residual temperature, Δt_{rs}' = duration below field residual temperate.

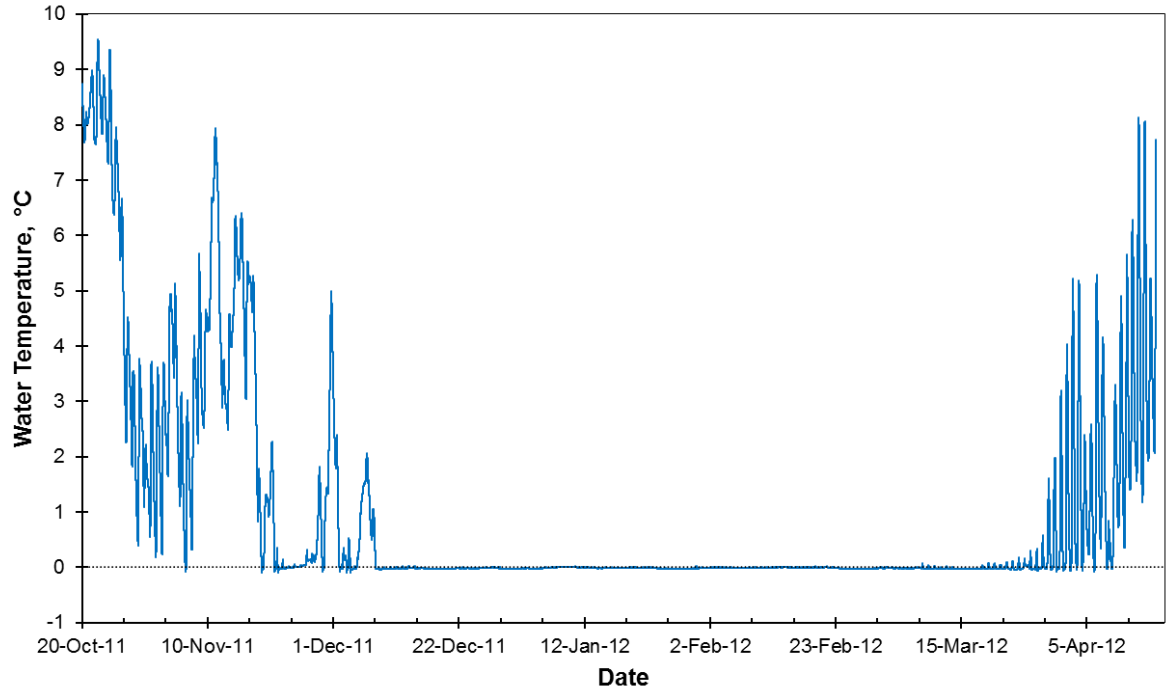

Fig 10. Cold season water temperatures at site G1 in the unregulated Gulquac River in New Brunswick, Canada.

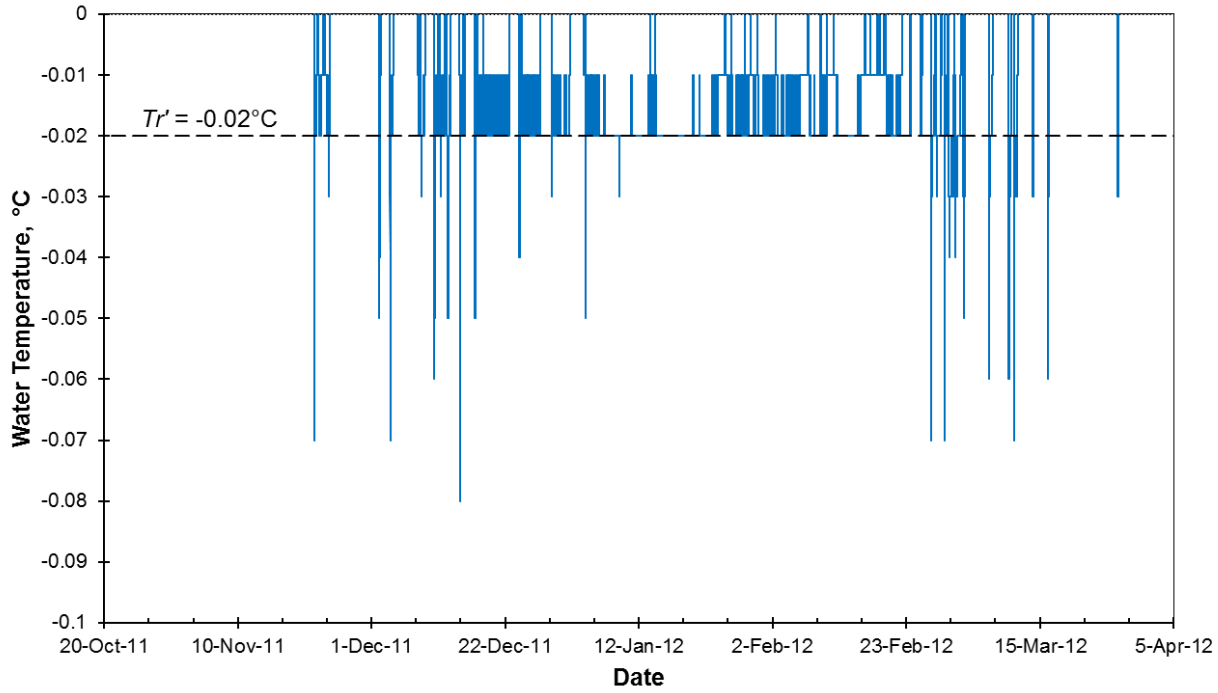

Fig 11. Water temperature at supercooling scale at Site D3 in the regulated River Dee in New Brunswick, Canada showing a field residual supercooling temperature (T_r') of -0.02°C and several supercooling events.

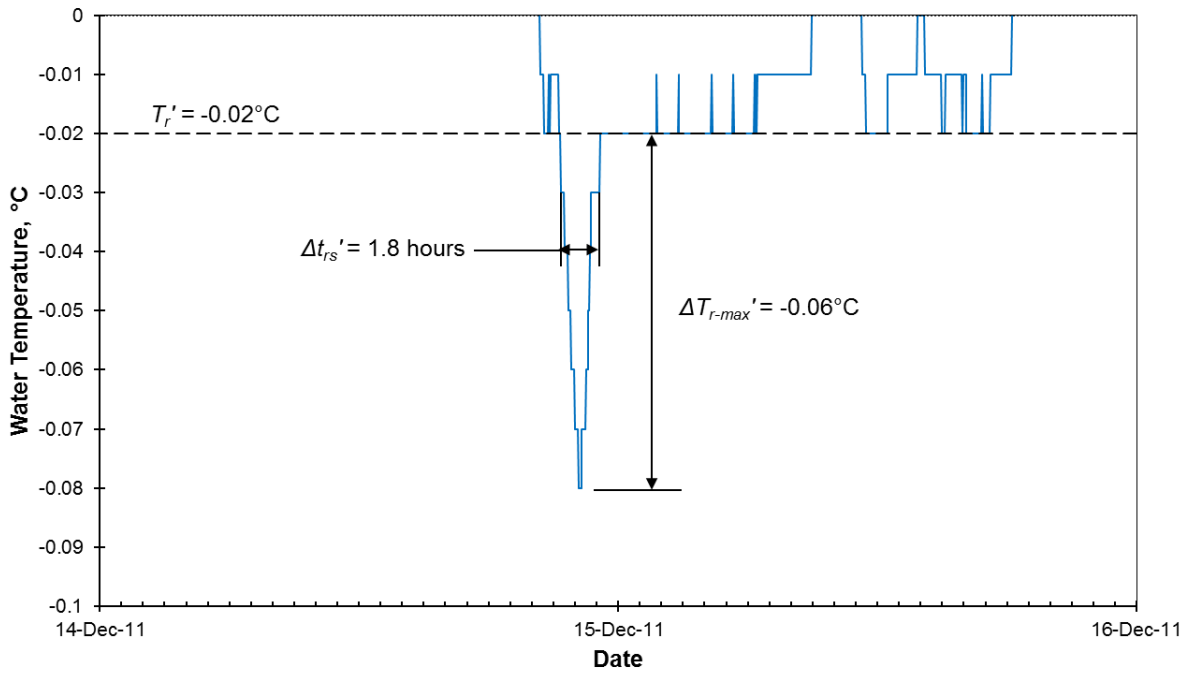

Fig 12. Surface water temperature at supercooling scale at Site D3 in the regulated River Dee in New Brunswick, Canada showing a single supercooling event field residual supercooling temperature (T_r') a maximum supercooling below field residual supercooling temperature ($\Delta T_{r\text{-}max}$') and duration of temperatures below field residual supercooling temperature (Δt_{rs}').

a)

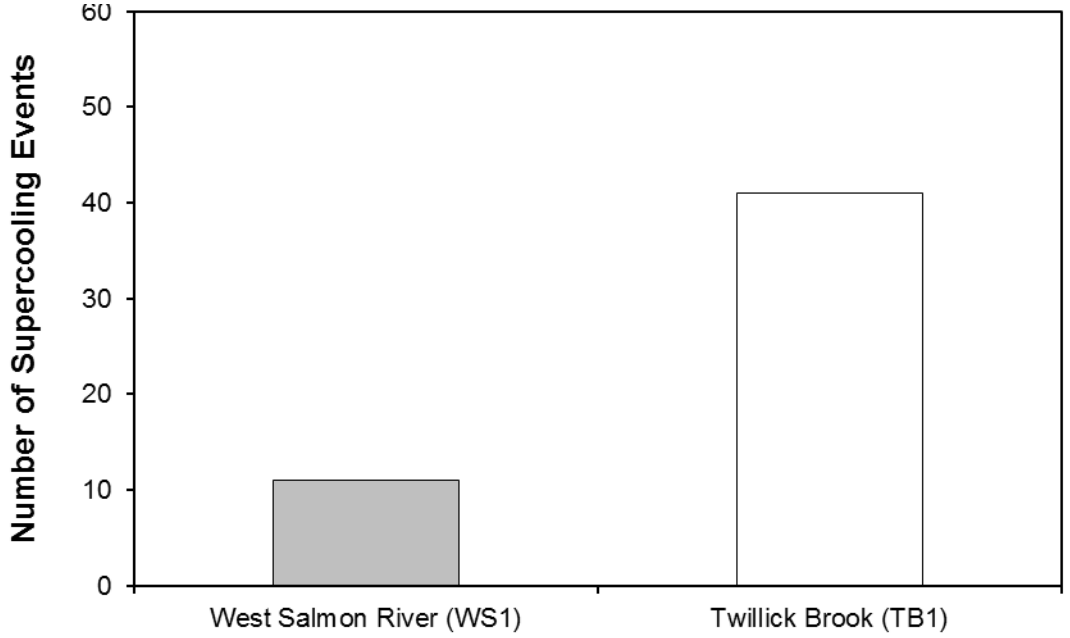

b)

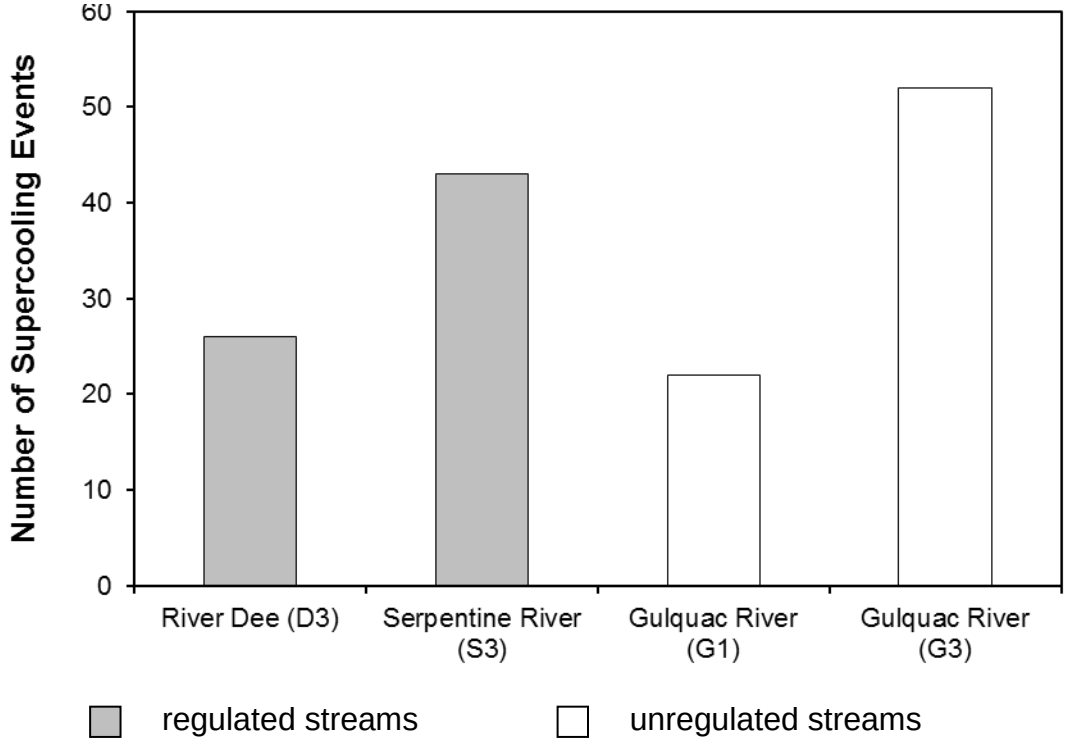

Figure 13. Number of supercooling events observed in a) the Newfoundland study streams, and b) the New Brunswick study streams.

a)

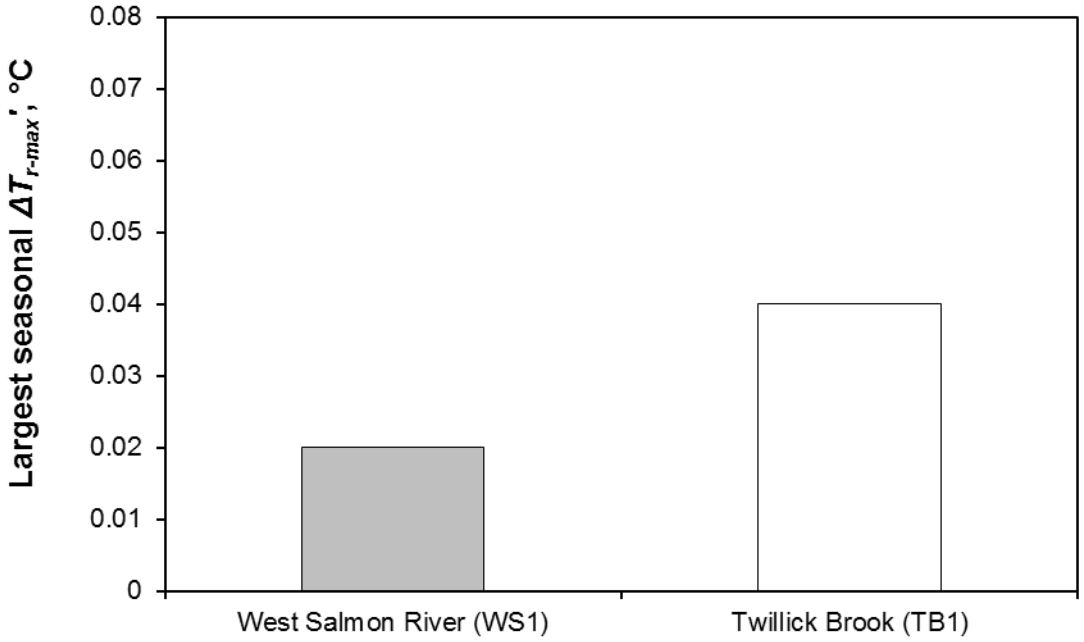

b)

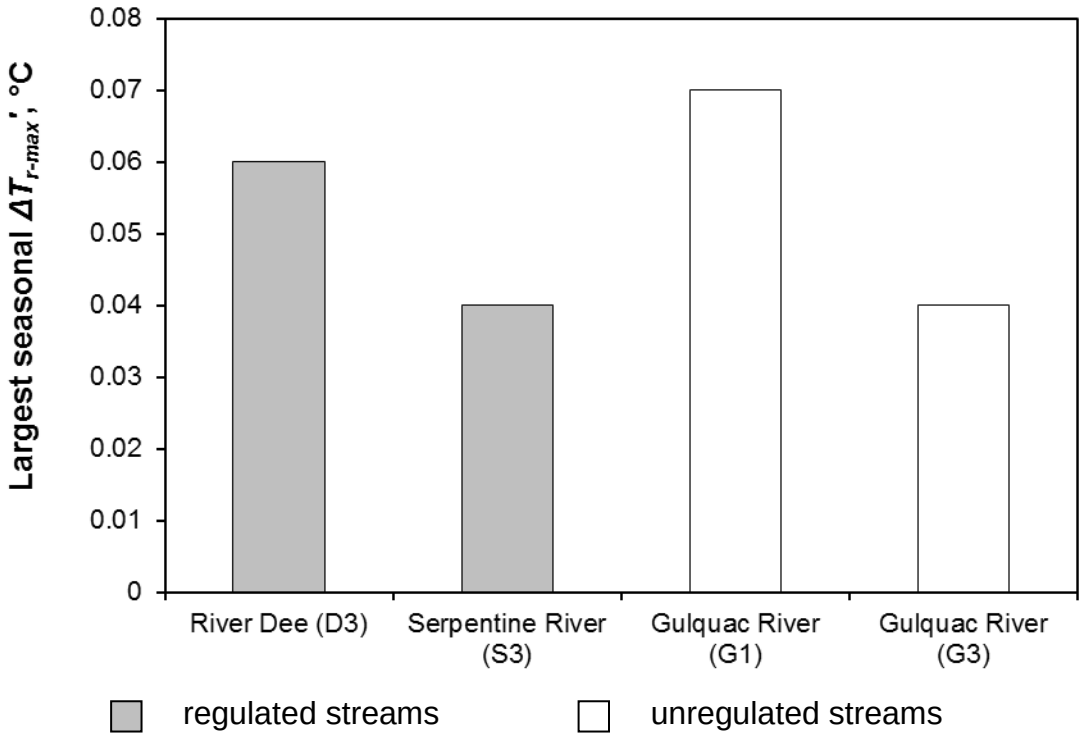

Figure 14. Largest supercooling below field supercooling temperaute ($\Delta T_{r\text{-}max}$') observed through the winter season in a) the Newfoundland study streams, and b) the New Brunswick study streams.

a)

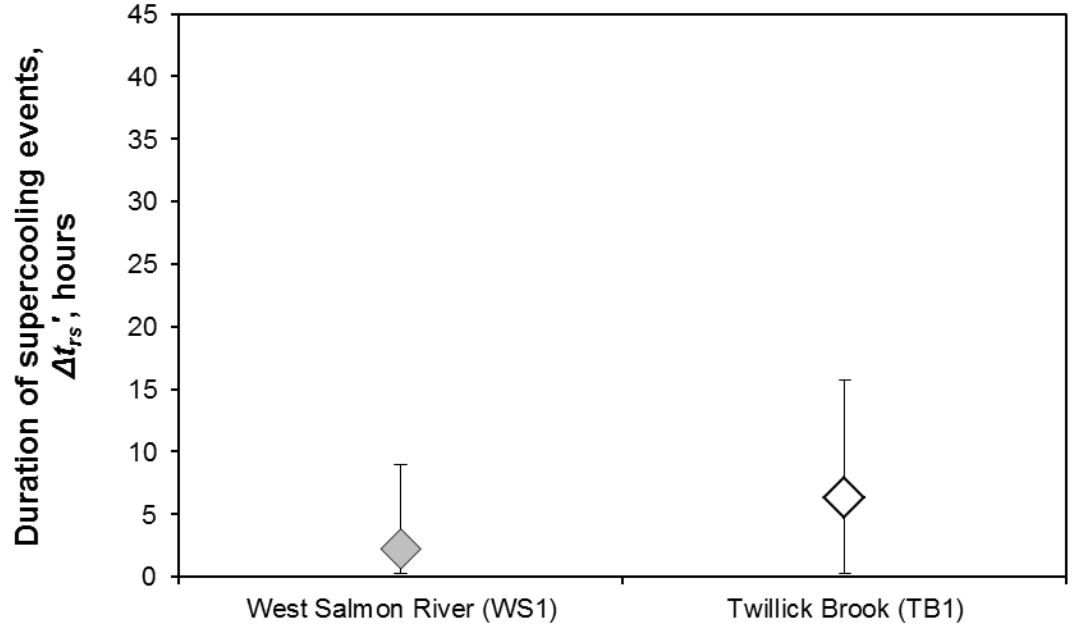

b)

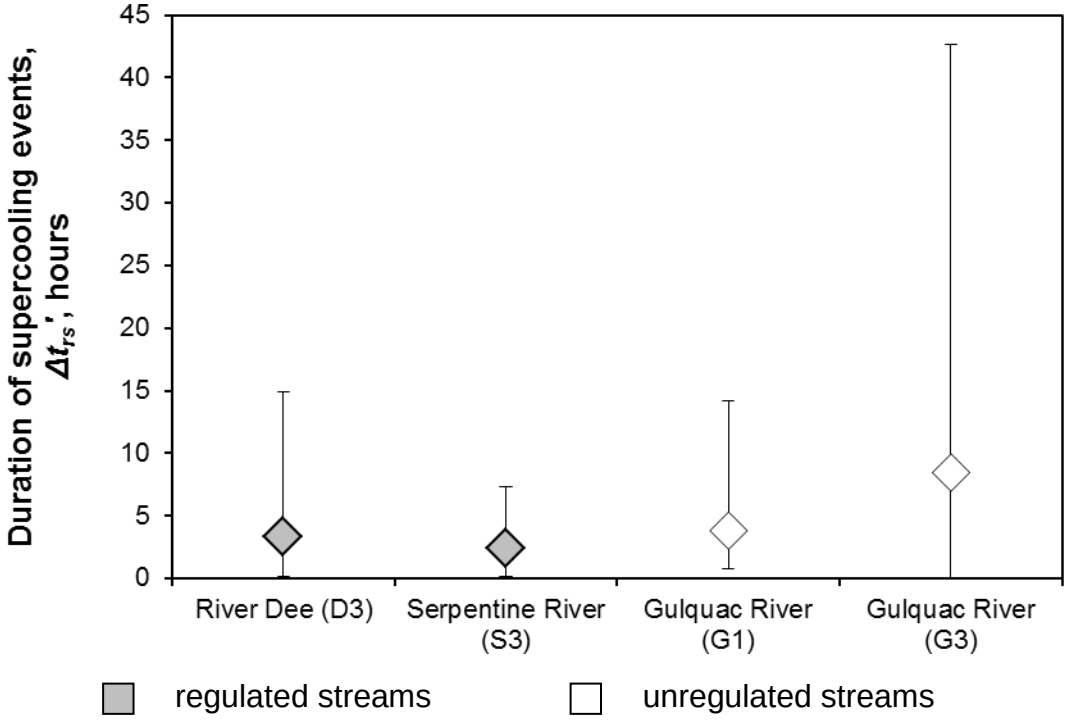

Figure 15. Duration of supercooling events (Δ_{trs}') in a) the Newfoundland study streams, and b) the New Brunswick study streams; error bars show maximum and minimum values.

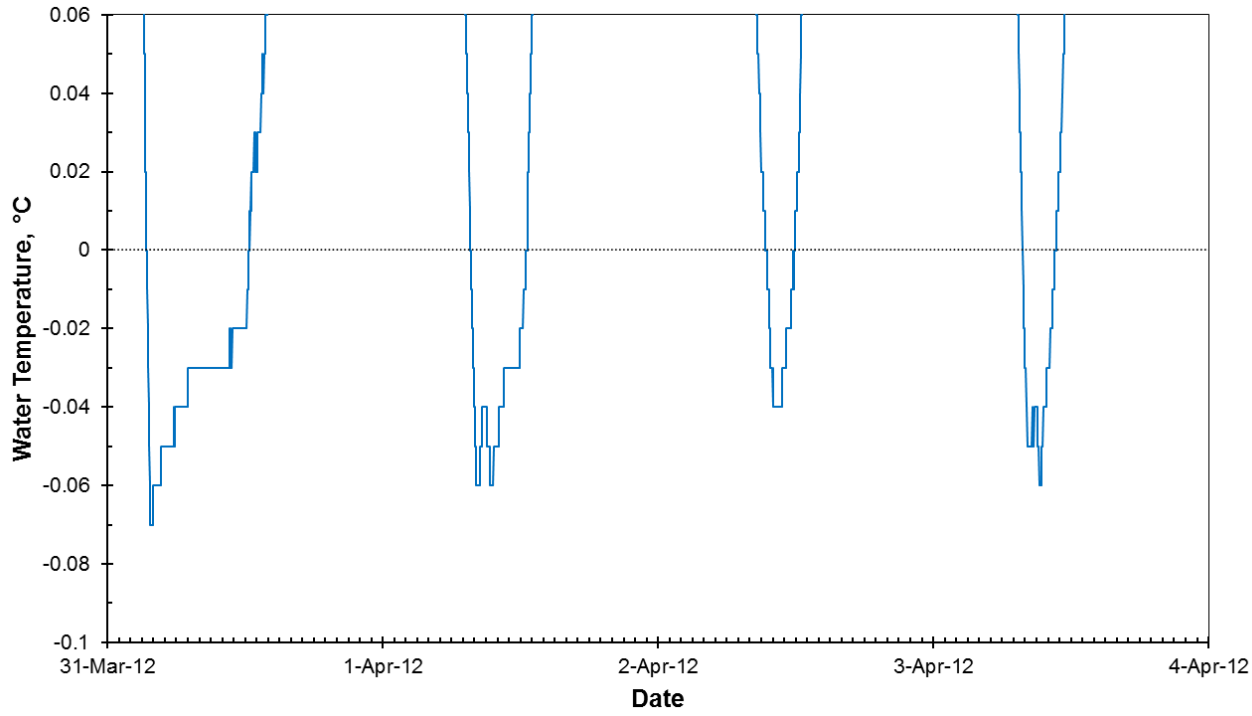

Fig 16. Water temperature at supercooling scale at Site G1 in the unregulated Gulquac River in New Brunswick, Canada showing a several spring supercooling events, and the fact that the field residual supercooling temperature (T_r') cannot be determined without additional data.